

Spatial distribution of multiple sclerosis lesions in the cervical spinal cord

Dominique Eden,^{1,*} Charley Gros,^{1,*} Atef Badji,^{1,2} Sara M. Dupont,^{1,3} Benjamin De Leener,¹ Josefina Maranzano,^{4,5} Ren Zhuoquiong,⁶ Yaou Liu,^{6,7} Tobias Granberg,^{8,9} Russell Ouellette,^{8,9} Leszek Stawiarz,⁸ Jan Hillert,⁸ Jason Talbott,³ Elise Bannier,^{10,11} Anne Kerbrat,^{11,12} Gilles Edan,^{11,12} Pierre Labauge,¹³ Virginie Callot,^{14,15} Jean Pelletier,^{15,16} Bertrand Audoin,^{15,16} Henitsoa Rasoanandrianina,^{14,15} Jean-Christophe Brisset,¹⁷ Paola Valsasina,¹⁸ Maria A. Rocca,¹⁸ Massimo Filippi,¹⁸ Rohit Bakshi,¹⁹ Shahamat Tauhid,¹⁹ Ferran Prados,^{20,21} Marios Yiannakas,²⁰ Hugh Kearney,²⁰ Olga Ciccarelli,²⁰ Seth A. Smith,²² Constantina Andrada Treaba,⁹ Caterina Mainero,⁹ Jennifer Lefeuvre,²³ Daniel S. Reich,²³ Govind Nair,²³ Timothy M. Shepherd,²⁴ Erik Charlson,²⁴ Yasuhiko Tachibana,²⁵ Masaaki Hori,²⁶ Kouhei Kamiya,²⁶ Lydia Chougar,^{26,27} Sridar Narayanan⁴ and Julien Cohen-Adad^{1,2,28}

*These authors contributed equally to this work.

Spinal cord lesions detected on MRI hold important diagnostic and prognostic value for multiple sclerosis. Previous attempts to correlate lesion burden with clinical status have had limited success, however, suggesting that lesion location may be a contributor. Our aim was to explore the spatial distribution of multiple sclerosis lesions in the cervical spinal cord, with respect to clinical status. We included 642 suspected or confirmed multiple sclerosis patients (31 clinically isolated syndrome, and 416 relapsing-remitting, 84 secondary progressive, and 73 primary progressive multiple sclerosis) from 13 clinical sites. Cervical spine lesions were manually delineated on T₂- and T₂*-weighted axial and sagittal MRI scans acquired at 3 or 7 T. With an automatic publicly-available analysis pipeline we produced voxelwise lesion frequency maps to identify predilection sites in various patient groups characterized by clinical subtype, Expanded Disability Status Scale score and disease duration. We also measured absolute and normalized lesion volumes in several regions of interest using an atlas-based approach, and evaluated differences within and between groups. The lateral funiculi were more frequently affected by lesions in progressive subtypes than in relapsing in voxelwise analysis ($P < 0.001$), which was further confirmed by absolute and normalized lesion volumes ($P < 0.01$). The central cord area was more often affected by lesions in primary progressive than relapse-remitting patients ($P < 0.001$). Between white and grey matter, the absolute lesion volume in the white matter was greater than in the grey matter in all phenotypes ($P < 0.001$); however when normalizing by each region, normalized lesion volumes were comparable between white and grey matter in primary progressive patients. Lesions appearing in the lateral funiculi and central cord area were significantly correlated with Expanded Disability Status Scale score ($P < 0.001$). High lesion frequencies were observed in patients with a more aggressive disease course, rather than long disease duration. Lesions located in the lateral funiculi and central cord area of the cervical spine may influence clinical status in multiple sclerosis. This work shows the added value of cervical spine lesions, and provides an avenue for evaluating the distribution of spinal cord lesions in various patient groups.

1 NeuroPoly Lab, Institute of Biomedical Engineering, Polytechnique Montreal, Montreal, QC, Canada

2 Department of Neuroscience, Faculty of Medicine, University of Montreal, Montreal, QC, Canada

- 3 Department of Radiology and Biomedical Imaging, Zuckerberg San Francisco General Hospital, University of California, San Francisco, CA, USA
- 4 McConnell Brain Imaging Centre, Montreal Neurological Institute, Montreal, Canada
- 5 Department of Anatomy, Université de Québec à Trois-Rivières, Trois-Rivières, QC, Canada
- 6 Department of Radiology, Xuanwu Hospital, Capital Medical University, Beijing 100053, P. R. China
- 7 Department of Radiology, Beijing Tiantan Hospital, Capital Medical University, Beijing 100050, P. R. China
- 8 Department of Clinical Neuroscience, Karolinska Institutet, Stockholm, Sweden
- 9 Massachusetts General Hospital, Boston, USA
- 10 CHU Rennes, Radiology Department, Rennes, France
- 11 Univ Rennes, CNRS, Inria, Inserm, IRISA UMR 6074, EMPENN - ERL U 1228, F-35000 Rennes, France
- 12 CHU Rennes, Neurology Department, Rennes, France
- 13 MS Unit, Department of Neurology, University Hospital of Montpellier, Montpellier, France
- 14 Aix Marseille University, CNRS, CRMBM, Marseille, France
- 15 APHM, CHU Timone, CEMEREM, Marseille, France
- 16 APHM, Department of Neurology, CHU Timone, APHM, Marseille
- 17 Observatoire Français de la Sclérose en Plaques (OFSEP) ; Université de Lyon, Université Claude Bernard Lyon 1; Hospices Civils de Lyon; CREATIS-LRMN, UMR 5220 CNRS and U 1044 INSERM; Lyon, France
- 18 Neuroimaging Research Unit, INSPE, Division of Neuroscience, San Raffaele Scientific Institute, Vita-Salute San Raffaele University, Milan, Italy
- 19 Brigham and Women's Hospital, Harvard Medical School, Boston, USA
- 20 Queen Square MS Centre, UCL Institute of Neurology, Faculty of Brain Sciences, University College London, London, UK
- 21 Center for Medical Image Computing (CMIC), Department of Medical Physics and Biomedical Engineering, University College London, London, UK
- 22 Vanderbilt University Institute of Imaging Science, Vanderbilt University Medical Center, Nashville, TN, USA
- 23 National Institute of Neurological Disorders and Stroke, National Institutes of Health, Maryland, USA
- 24 Department of Radiology, NYU Langone Medical Center, New York, USA
- 25 National Institute of Radiological Sciences, Chiba, Chiba, Japan
- 26 Department of Radiology, Juntendo University School of Medicine, Tokyo, Japan
- 27 Hospital Cochin, Paris, France
- 28 Functional Neuroimaging Unit, CRIUGM, Université de Montréal, Montreal, QC, Canada

Correspondence to: Julien Cohen-Adad

Dept. Genie Electrique, L5610, Ecole Polytechnique, 2900 Edouard-Montpetit Bld, Montreal QC, H3T 1J4, Canada

E-mail: jcohen@polymtl.ca; Skype: jcohenadad

Keywords: multiple sclerosis; spinal cord; lesions; multicentre; MRI

Abbreviations: CIS = clinically isolated syndrome; EDSS = Expanded Disability Status Scale; MSSS = Multiple Sclerosis Severity Score; PPMS = primary progressive multiple sclerosis; RRMS = relapsing-remitting multiple sclerosis; SPMS = secondary progressive multiple sclerosis

Introduction

Multiple sclerosis is a chronic autoimmune disease of the CNS characterized by pathologically heterogeneous abnormalities disseminated in both space and time. For several decades, MRI has proven a powerful diagnostic tool and monitor of disease progression (Filippi and Rocca, 2007; Absinta *et al.*, 2016; Kaunzner and Gauthier, 2017) by facilitating detection of brain and spinal lesions (Fazekas *et al.*, 1999). Studies have revealed that MRI of the spinal cord in particular, holds important value for diagnosis and prognosis of multiple sclerosis at clinical presentation (Lycklama *et al.*, 2003; Sombekke *et al.*, 2013; Kearney *et al.*, 2015b; Brownlee *et al.*, 2017; Arrambide *et al.*, 2018). It has also been established that spinal lesions are more often associated with sensorimotor symptoms than brain lesions in progressive forms of the

disease (Filippi *et al.*, 2000; Rovaris *et al.*, 2000). Despite this, focus on lesions in the spinal cord has been less prevalent than in the brain, likely owing to the inherent technical challenges associated with imaging a small, mobile structure (Kearney *et al.*, 2015b). Recent advancements in MRI technology have reported higher specificity in visualizing spinal cord pathology, with T₂-weighted conventional MRI demonstrating good performance in the identification of lesions (Filippi and Rocca, 2007; Weier *et al.*, 2012; Kearney *et al.*, 2013; Stroman *et al.*, 2014; Gass *et al.*, 2015; Breckwoldt *et al.*, 2017). At present, however, correlation between lesion burden and clinical presentation remains modest in the spinal cord (Kidd *et al.*, 1993; Nijeholt *et al.*, 1998; Stankiewicz *et al.*, 2009), suggesting that lesion location may play a greater role in the development of clinical symptoms. Studies have shown that lesions occur in cervical portions of the cord more frequently than

thoracolumbar (Oppenheimer, 1978; Goldin and Kantor, 2008b; Weier *et al.*, 2012; Hua *et al.*, 2015); however, several studies show conflicting results in the distribution across vertebral levels (Oppenheimer, 1978; Kidd *et al.*, 1993; Rocca *et al.*, 2013; Hua *et al.*, 2015; Kearney *et al.*, 2015b). It has also been reported that whilst lateral and posterior regions of the white matter are more affected than the anterior region and central cord area (Fog, 1950; Oppenheimer, 1978; Nijeholt *et al.*, 2001; Lycklama *et al.*, 2003; Gilmore *et al.*, 2009b; Weier *et al.*, 2012; Gass *et al.*, 2015; Kearney *et al.*, 2016; Valsasina *et al.*, 2018), lesions do not spare the grey matter (Gilmore *et al.*, 2009b; Weier *et al.*, 2012; Gass *et al.*, 2015; Kearney *et al.*, 2016; Schmierer *et al.*, 2018). Few studies, however, have attempted to identify predilection sites of spinal lesions with respect to phenotype (Rocca *et al.*, 2013; Valsasina *et al.*, 2018) or disability score (Rocca *et al.*, 2013; Valsasina *et al.*, 2018), and none with respect to disability score accounting for disease duration.

In this present study, we aimed to extend these findings by using a comprehensive atlas-based method to study the spatial distribution of cervical spine lesions in patients characterized by clinical status. We produced voxelwise lesion frequency maps and measured MRI lesions burden in several regions of interest, from a multicentre cohort, and evaluated differences within and between patient populations characterized by clinical subtype, Expanded Disability Status Scale (EDSS) score and disease duration.

Materials and methods

Subjects

A total of 642 patients with multiple sclerosis or suspected multiple sclerosis were retrospectively included in this study. Inclusion criteria consisted of age > 18 years and a diagnosis of clinically isolated syndrome (CIS), relapsing-remitting multiple sclerosis (RRMS), secondary progressive multiple sclerosis (SPMS), or primary progressive multiple sclerosis (PPMS). Patients diagnosed with degenerative cervical myelopathy, spinal cord trauma or neuroinflammatory diseases other than multiple sclerosis were excluded from the study, as well as patients with MRI images where cervical cord lesions could not be reliably segmented because of excessive imaging artefacts or poor quality. This research was approved by the local institutional review board, and informed written consent was obtained from all participants.

MRI data acquisition

Scans were acquired on 3 T and 7 T MRI systems (Philips or Siemens), with varying protocol across sites (Supplementary Table 1). The sequences acquired, as well as median and range for some parameters, were: (i) axial T₂- or T₂*-weighted ($n = 642$), median in-plane resolution (range): $0.47 \times 0.47 \text{ mm}^2$ ($0.29 \times 0.29 \text{ mm}^2$ – $0.84 \times 0.84 \text{ mm}^2$); median slice thickness (range): 3.60 mm (2.50–6.00 mm); and (ii) sagittal T₂-weighted ($n = 470$), median in-plane resolution (range):

$0.68 \times 0.68 \text{ mm}^2$ ($0.41 \times 0.41 \text{ mm}^2$ – $1.00 \times 1.00 \text{ mm}^2$); median slice thickness (range): 2.75 mm (1.00–5.2 mm).

All subjects had at least one axial scan and full coverage of the cervical cord in at least one orientation.

MRI data processing

Data were processed with an automatic publicly-available pipeline based on tools from the Spinal Cord Toolbox v3.0 (Lévy *et al.*, 2015; De Leener *et al.*, 2016) (Fig. 1).

Generation of cord and lesion masks

Cervical cord masks were automatically generated by identifying the cord centerline using OptiC (Gros *et al.*, 2017) and segmentation using PropSeg (De Leener *et al.*, 2014). Masks were then reviewed by two raters (D.E., C.G.) and manually adjusted with FMRIB Software Library (FSL) viewer (Jenkinson *et al.*, 2012) in slices presenting low contrast difference between the cord and CSF. Binary lesion masks were manually generated on both axial and sagittal scans by nine raters, including radiologists (J.M., J.T., M.H., Y.T., R.Z., L.C.) and experienced readers (A.B., R.O., T.G.) using ITK-SNAP Toolbox 3.6.0 (Yushkevich *et al.*, 2006). For instances where lesions were not detected, an empty lesion mask was generated ($n = 56$). All raters were blinded to the diagnosis and clinical information. To examine lesion segmentation inter-rater reliability, all raters repeated segmentations on a randomized subset of patients ($n = 10$) blinded to previous assessment. For each patient image, a consensus reading was produced using majority voting. Dice's Kappa (Dice, 1945), lesion positive predictive value and lesion sensitivity measures were also computed (Commowick *et al.*, 2018). In brief, a true positive was considered when a rater's segmentation overlapped with the consensus reading by at least 50%.

Registration to the PAM50 template

A multi-step registration method based on non-linear transformations was used to register each magnetic resonance scan to the PAM50-T₂ spinal cord template (De Leener *et al.*, 2018), performed on a slice-wise basis with parameters tailored to this study. Quality of MRI registration were approved by visual inspection (D.E., C.G.). The same non-linear transformation from each registration (coupled with linear interpolation) was applied to cord and lesion masks, co-registering all data to a common space. For subjects with both axial and sagittal data, a weighted lesion mask was produced by voxel-wise averaging of both orientations.

Generation of lesion frequency maps

Cervical spine lesion frequency maps were produced in the template space for a given cohort, by dividing the sum of weighted lesion masks by the sum of cord masks on a voxel-wise basis. Voxel intensities represented the frequency of a lesion (%) occurring at the corresponding voxel coordinate.

MRI data analysis

Lesion count, total lesion volume, and individual lesion volume were measured for each subject, using weighted lesion masks in the template space. In this study, individual

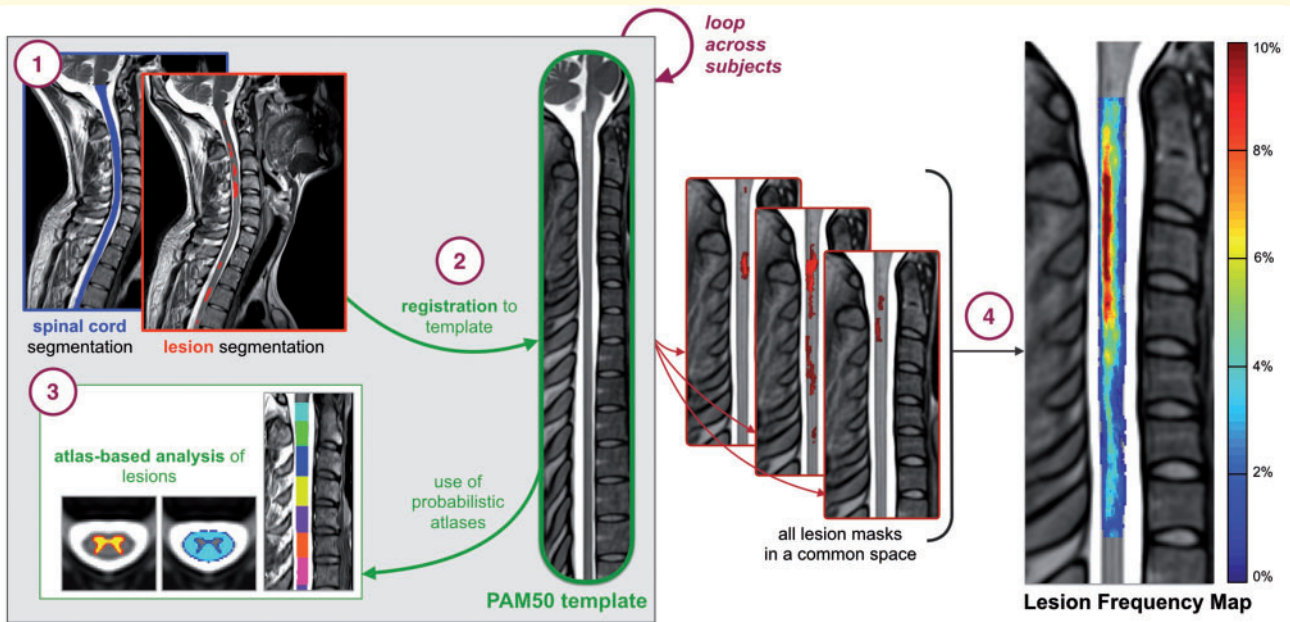


Figure 1 Illustration of the automated analysis pipeline. (1) Generation of binary cord and lesion masks. (2) Registration to the PAM50 template. (3) Use of probabilistic atlases to compute lesion characteristics. (4) Weighted lesion masks in the template space to produce a lesion frequency map.

lesion volume refers to the volume of each distinct lesion. The cord cross-sectional area was also measured, using cord masks in the native space with geometric adjustment to account for cord curvature. To ensure that lesion characteristics measured in the template space produced the same result as those in the native space, the total lesion volume was computed for 10 randomly selected subjects in both the native and template space. Lesion frequency maps were produced for the whole cohort, patients grouped by clinical subtype, and patients grouped by EDSS score categories (mild: 0–2.5; moderate: 3–5.5; severe: ≥ 6) and further subgrouped by disease duration categories (short: 0–5 years; moderate: 5–15; long: ≥ 15). EDSS score ranges were chosen in accordance with benchmarks of disability accumulation in multiple sclerosis (Kurtzke, 1983).

Absolute lesion volume and normalized lesion volume were measured in various regions of interest for each subject, using probabilistic atlases (Lévy *et al.*, 2015). In this study, absolute lesion volume refers to the total lesions volume within a region and normalized lesion volume refers to the total lesion volume within a region normalized to the volume of the region, therefore indicating the proportion of tissue affected by lesions in the respective region. If, for example, a region of 1000 mm³ is affected by lesions covering 100 mm³, the effective normalized lesion volume would be 0.10. Lesion appearance was measured in: (i) white and grey matter; (ii) dorsal column, lateral funiculi and ventral funiculi; (iii) sensory and motor tracts, across the full length of the cervical cord; and (iv) the whole cord corresponding to each cervical vertebral level, C1–C7. Predilection sites were quantified within and between patients grouped by phenotype, EDSS score categories, and ranges of Multiple Sclerosis Severity Score (MSSS) (Roxburgh *et al.*, 2005). For analyses involving grey matter, analyses were performed exclusively on patients with full cervical axial T₂-

weighted images ($n = 231$) due to the difficulty of detecting grey matter lesions in T₂*-weighted images.

Statistical analysis

Comparisons within and between patient groups were performed using *t*-test for normally distributed data, and Mann-Whitney U-test for non-parametric data. Correlations between EDSS score and lesion measures were determined using Spearman's rank correlation coefficient. Multiple regression analysis was used to evaluate the influence of age, gender, disease duration and cross-sectional area. Statistical significance was thresholded at $P < 0.05$. Non-parametric permutation based cluster analyses were performed to statistically infer voxelwise lesion frequency maps, using FMRIB Software Library's *Randomise* function (Smith *et al.*, 2004) with 5000 permutations. Voxelwise comparisons between phenotypes, corrected for age, were performed to identify differences in lesion location, and voxelwise correlation, adjusted for age and disease duration, was performed to determine lesion locations associated with an increased EDSS score. Significant clusters of voxels were identified with threshold-free cluster enhancement (Smith and Nichols, 2009) at $P < 0.05$, using family-wise error correction for multiple comparisons. Anatomical locations of significant clusters were determined using PAM50 atlas coordinates.

Data availability

Guidelines for manual lesion segmentation, inter-rater reliability script, processing scripts and generated lesion frequency maps are available at: <https://osf.io/cx5ur/>. The authors confirm that the data supporting the findings of this study are available within the article, Supplementary material, and public data repository.

Results

Table 1 shows demographics and clinical information. The EDSS scores were similar for patients with SPMS and PPMS; however, MSSS scores were higher for PPMS than for SPMS ($P < 0.05$). Table 2 presents lesion count, total lesion volume, and individual lesion load measures across the full cervical cord. No cervical spine lesions were identified in 22.58% ($n = 7$) of CIS patients, 9.62% ($n = 40$) of RRMS patients, 4.76% ($n = 4$) of SPMS patients, and 1.37% ($n = 1$) of PPMS patients. Lesion count and total lesion volume was lower in CIS patients than in RRMS, SPMS and PPMS patients ($P < 0.01$). Compared to RRMS patients, lesion count was higher in SPMS ($P < 0.01$) and PPMS ($P < 0.05$) patients. Remaining comparisons were not significant ($P > 0.05$). Overall, inter-rater agreement was good with Dice kappa of 0.63 ± 0.21 , lesion positive predictive value of 0.79 ± 0.16 and lesion sensitivity of 0.69 ± 0.16 . For ensuring measures were equivalent between template and native spaces, the average total lesion volume across 10 randomly selected subjects was 238.52 mm^3 in the template space and 238.04 mm^3 in the native space, yielding a relative difference of 0.75%.

In multiple regression analysis, lesion count explained 44% of the variance in EDSS score and total lesion volume explained 43%. Age, gender, disease duration and cross-sectional area of the cord were significant contributors to the models. When removing cross-sectional area from the models, lesion count and total lesion volume explained 35 and 36% of the variance in EDSS score, respectively. No significant effect of individual lesion volume was found.

Lesion frequency maps

Lesions were more frequent in upper cervical cord (C1–C3) than in the lower (C4–C7) when observed across all patients (Fig. 2). In general, lesion appeared to affect the dorsal column most followed by the lateral funiculi, where highest frequencies were observed in the centre of these regions.

Between phenotypes, lesions occurred less in CIS patients than in RRMS, SPMS and PPMS patients (Fig. 3). In all groups, lesions affected C2 and C3 vertebral levels more than other cervical vertebral levels. Locations of high

frequency appeared to be sporadic throughout the cervical cord in CIS patients. For remaining groups, frequencies $>10\%$ were observed in the dorsal region for RRMS patients, the dorsal and lateral regions for SPMS patients and the dorsal, lateral and central regions of the cord for PPMS patients, particularly at C3 vertebral level.

Voxelwise comparisons confirmed that lesion frequency was higher in SPMS than RRMS patients, with significant clusters in the lateral funiculi of C3 vertebral level (peak t -value: 4.5, $P < 0.05$). At the voxel location where maximum pseudo- t -value was observed, a lesion was present in 9.7% of SPMS patients, and 4.4% of RRMS. Lesion frequency was also higher in PPMS than RRMS patients, with significant clusters observed in the lateral funiculi (peak t -value: 5.0) and central region (peak t -value: 4.3) at C3, $P < 0.05$. Lesions affected 6.7% of PPMS versus 2.6% of RRMS patients at location of maximum pseudo- t -value. No voxel clusters were found significantly different between SPMS and PPMS patients.

In patients grouped by EDSS score categories and further subgrouped by disease duration, regions of highest lesion frequency were not the same for all groups (Fig. 4). In most groups, the dorsal portion of the cervical cord was most affected by lesions; however, in patients with severe EDSS scores and short disease durations, the dorsal, lateral, and central regions, were similarly affected. In the mild EDSS score group, an increased lesion frequency was observed in groups with longer disease durations. Conversely, in moderate and severe EDSS score groups, an increased lesion frequency was observed in groups with shorter disease durations. It was also observed that in a given disease duration category (Fig. 4), the lesion frequency tended to increase with EDSS score severity.

Voxelwise analysis showed that EDSS score, adjusted for age and disease duration, correlated with lesion frequency in lateral and central regions. Significant clusters were observed in the lateral funiculi and central regions at C1 (peak t -value: 5.2), C2 (peak t -value: 5.4) and C3 (peak t -value: 5.5), and the lateral funiculi at C4 (peak t -value: 4.3), $P < 0.001$, and C5 (peak t -value: 3.7), $P < 0.01$. Supplementary Table 4 shows results for voxelwise between-group comparisons for phenotypic distributions, and correlation with EDSS score.

Lesion frequency maps for EDSS score categories are shown in Supplementary Fig. 1. For each map, mean

Table 1 Demographic and clinical data

	CIS <i>n</i> = 31	RRMS <i>n</i> = 416	SPMS <i>n</i> = 84	PPMS <i>n</i> = 73	All patients <i>n</i> = 642
Gender, female / male	22 / 10	293 / 150	49 / 34	39 / 36	411 / 231
Age, years, mean \pm SD	43.1 \pm 11.0	43.2 \pm 8.2	54.0 \pm 8.9	57.5 \pm 12.0	44.3 \pm 13.0
Disease duration, years, mean \pm SD	4.2 \pm 3.7	8.9 \pm 8.2	23.4 \pm 10.7	16.6 \pm 9.9	11.5 \pm 10.2
EDSS, median (range)	1.0 (0.0–3.5)	2.9 (0.0–8.0)	6.0 (2.5–8.0)	6.0 (1.0–8.5)	3.0 (0.0–8.5)
MSSS, median (range)	2.0 (0.2–7.3)	3.4 (0.0–9.8)	6.3 (1.3–9.0)	6.7 (0.8–9.6)	4.3 (0.1–9.8)

Demographic and clinical data were not available for all subjects.

Table 2 Cervical cord MRI lesion characteristics

		CIS <i>n</i> = 31	RRMS <i>n</i> = 416	SPMS <i>n</i> = 84	PPMS <i>n</i> = 73	All patients <i>n</i> = 642
Lesion count, <i>n</i>	Median (range)	1.0 (0.0–5.0)	2.0 (0.0–9.0)	3.0 (0.0–9.0)	3.0 (0.0–6.0)	2.0 (0.0–9.0)
Total lesion volume, mm ³	Mean	103.8	184.7	196.1	208.2	183.8
	Median	51.4	89.8	125.0	125.0	97.2
	IQR	108.6	209.1	139.6	170.9	191.9
	Range	(0.0–473.3)	(0.0–1511.7)	(0.0–1048.4)	(0.0–1677.2)	(0.0–1677.2)
Individual lesion volume, mm ³	Mean	76.2	100.8	96.5	102.6	99.5
	Median	44.6	46.7	45.4	41.9	45.3
	IQR	66.7	82.5	50.6	64.7	75.0
	Range	(2.8–473.3)	(0.2–1511.7)	(5.9–1048.4)	(4.9–1677.2)	(0.2–1677.2)
Cord cross-sectional area, mm ²	Mean	73.7	72.0	65.5	68.6	70.8
	Median	73.4	72.2	64.8	67.2	70.5
	IQR	8.6	15.8	11.7	10.8	15.7
	Range	(61.5–97.1)	(42.2–99.6)	(47.0–85.4)	(51.1–90.9)	(40.5–99.6)

Phenotype was not available for all subjects.

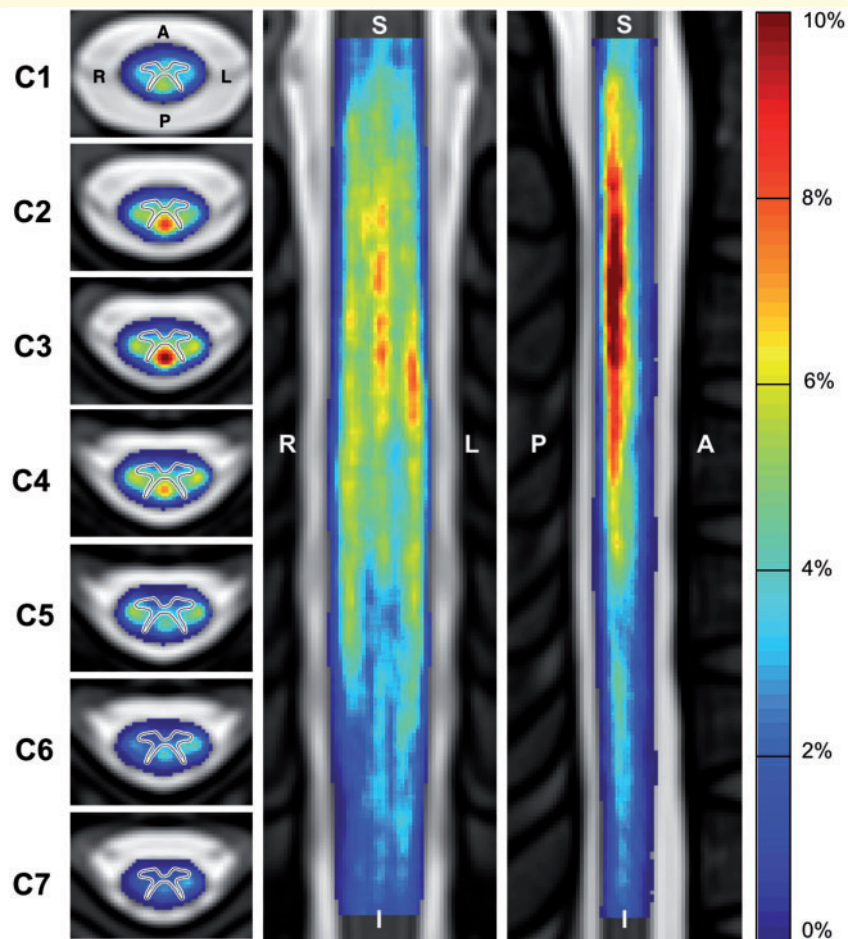


Figure 2 Frequency of multiple sclerosis lesions in the cervical spinal cord for all patients (*n* = 642). Frequency shown in axial (left), coronal (middle) and sagittal (right) view. Note that the axial view shows an average of the lesion frequency across each vertebral level. The grey matter contour has been overlaid on the axial view for clarity purposes. A = anterior; I = Inferior; L = left; P = posterior; R = right; S = superior.

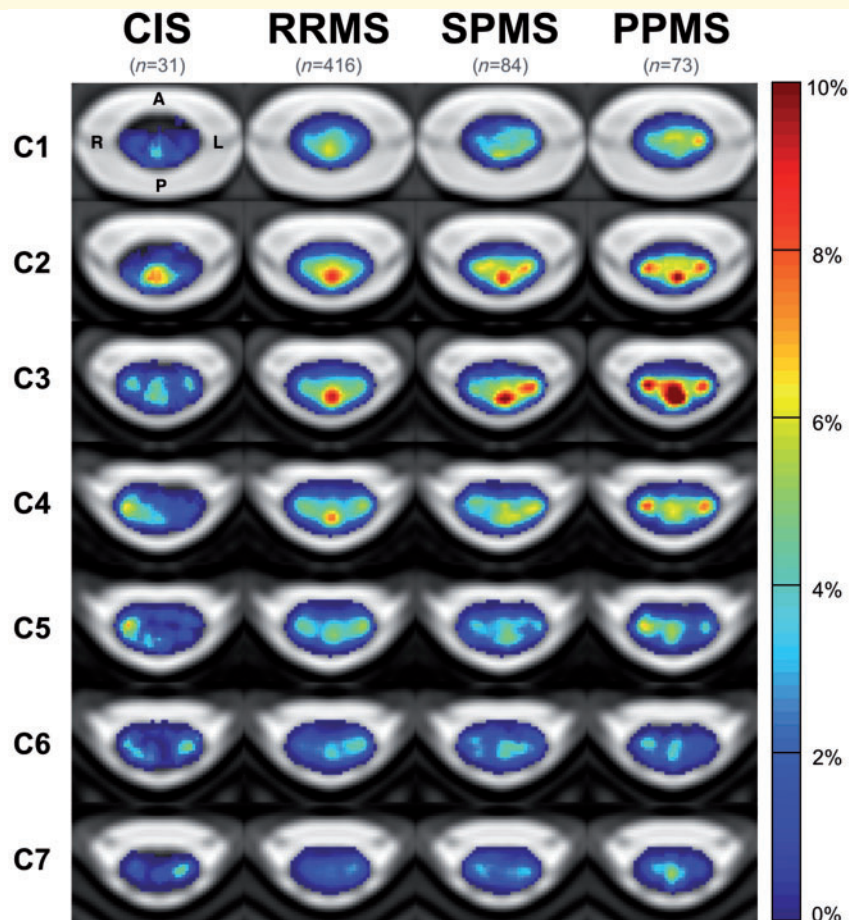


Figure 3 Frequency of multiple sclerosis lesions the cervical spinal cord for patients grouped by phenotype. A = anterior; L = left; P = posterior; R = right.

lesion frequencies for studied regions of interest are detailed in Supplementary Tables 2 and 3.

Absolute and normalized lesion volumes in regions of interest

The absolute lesion volume was greater in the white matter than in the grey matter when evaluating measures across all patients (median: 62.01 mm³ versus 11.09 mm³, $P < 0.001$). For all phenotype groups, absolute lesion volume was greater in the white matter than in the grey matter ($P < 0.001$, Fig. 5A). When normalizing by each region, the normalized lesion volume in white matter was also greater than in the grey matter for all groups. The normalized lesion volume in the grey matter was more comparable to white matter in progressive subtypes compared to other subtypes, where relative differences between regions were 86% for CIS, 28% for RRMS, 20% for SPMS and 13% for PPMS.

Between groups, absolute and normalized lesion volumes in cervical grey matter were less in CIS patients compared to RRMS ($P < 0.01$), SPMS and PPMS patients

($P < 0.001$), and less in RRMS compared to SPMS ($P < 0.05$). Absolute and normalized lesion volumes in cervical white matter were greater in SPMS and PPMS patients than in RRMS ($P < 0.01$) and in CIS ($P < 0.001$).

When evaluating regions in cervical white matter (Fig. 5B), both absolute and normalized lesion volumes were significantly greater in the dorsal column and lateral funiculi than in the ventral funiculi for CIS patients ($P < 0.01$), RRMS, SPMS and PPMS patients ($P < 0.001$). The absolute lesion volume was also greater in the lateral funiculi than in the dorsal column for PPMS patients ($P < 0.05$).

For assessing differences between groups, the dorsal column and ventral funiculi were less affected by lesions in CIS patients than other groups ($P < 0.01$). Patients with SPMS and PPMS were more affected by lesions in the lateral funiculi than patients with RRMS and CIS ($P < 0.01$). Patients with PPMS were also more impacted by lesions than RRMS patients in the ventral funiculi ($P < 0.05$).

In the rostrocaudal direction, the upper cervical was more impacted than the lower cervical cord across the whole cohort ($P < 0.001$, Fig. 5C). Cervical levels C2 and

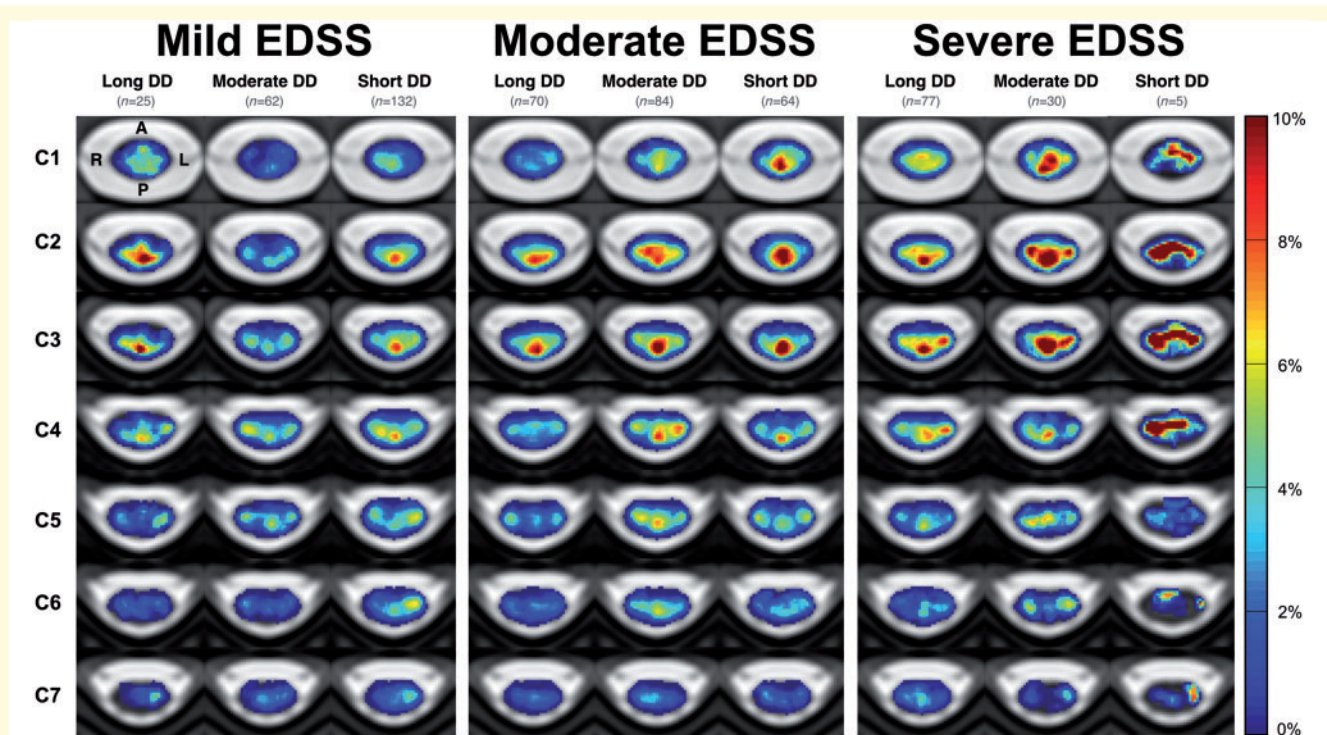


Figure 4 Frequency of multiple sclerosis lesions in the cervical spinal cord for patients grouped by ranges of EDSS score and disease duration. EDSS scores categories: mild (0–2.5), moderate (3–5.5) and severe (≥ 6), and sub-categorized by disease duration categories: short (0–5 years) moderate (5–15 years), long (≥ 15 years). Patients with a mild EDSS score and long disease duration may be considered as benign multiple sclerosis. A = anterior; DD = disease duration; L = left; P = posterior; R = right.

C3 were the most affected vertebral levels for all patient groups, and C7 was the least for all patient groups excluding CIS patients ($P < 0.001$). No other comparisons were significant.

Absolute and normalized lesion volumes corresponding to Fig. 5A and B are summarized in Supplementary Tables 5 and 6.

In patients grouped by ranges of EDSS score, sensory tracts were more affected by lesions than motor tracts in patients with mild and moderate EDSS scores ($P < 0.01$) and severe EDSS scores ($P < 0.05$).

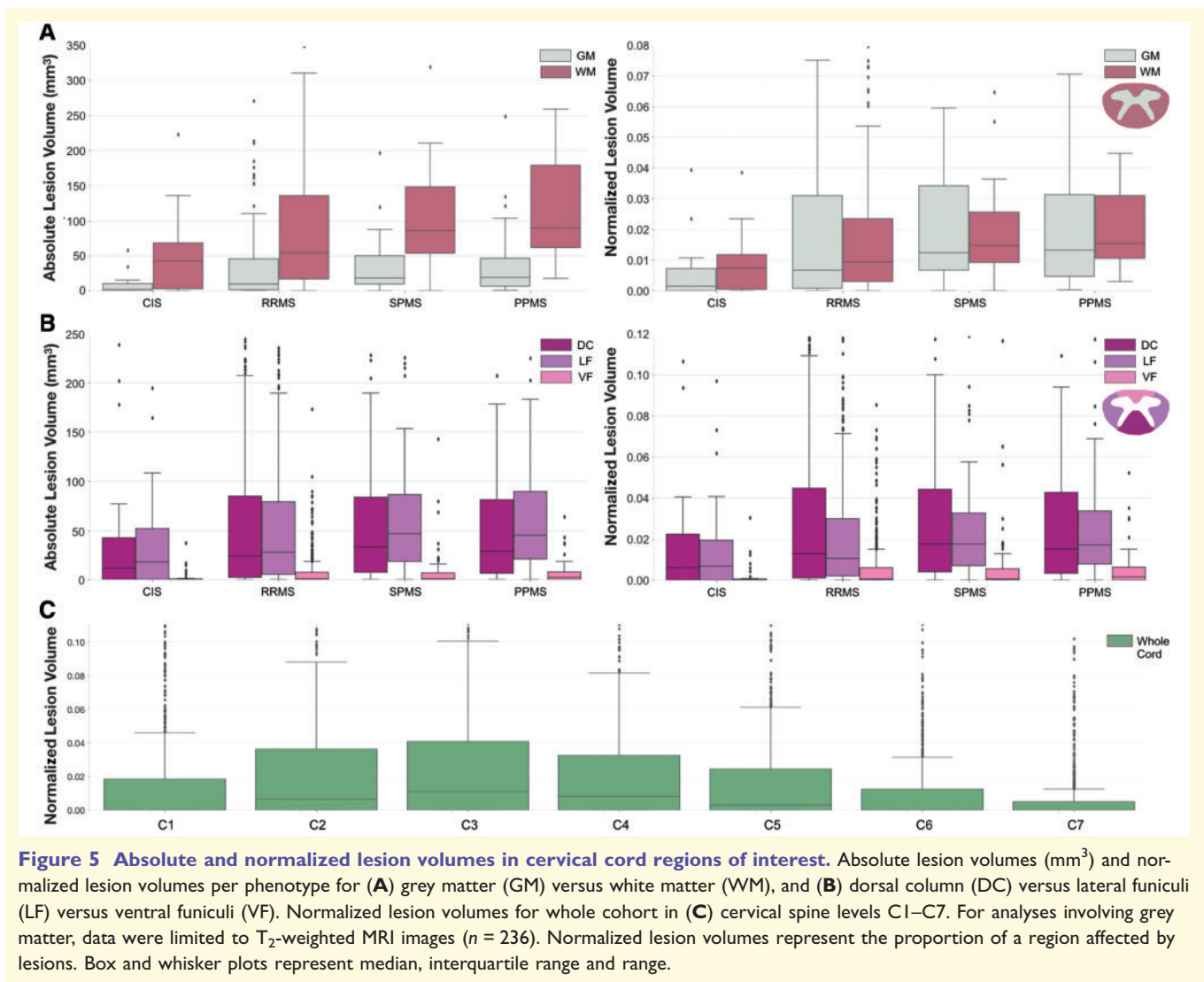
Between groups, patients with severe EDSS were more affected by lesions in motor tracts than patients with moderate ($P < 0.01$) and mild EDSS ($P < 0.001$). Lesions also affected sensory tracts more in patients with severe EDSS than with mild EDSS ($P < 0.01$), and moderate EDSS than with mild EDSS ($P < 0.05$), however no differences were detected between severe and moderate EDSS groups. Between moderate and severe groups, the severe EDSS group had 17% more lesion-affected volume in sensory tracts, and 40% more lesion-affected volume in motor tracts. Spearman correlation coefficients were 0.17 ($P < 0.001$) for motor tracts and 0.13 for sensory tracts ($P < 0.01$). In multiple regression analysis, the normalized lesion volume in motor tracts explained 44% of the variance in EDSS score, and normalized lesion volume in sensory tracts explained 43%. Absolute and normalized lesion

volumes corresponding to Fig. 6 are shown in Supplementary Table 7.

When grouping patients by MSSS score, patients with MSSS scores < 9.0 were also more impacted by lesions in sensory than in motor tracts (Fig. 6B). For patients with MSSS scores > 9.0 , motor tracts were 23% more occupied by lesions than sensory tracts. Comparisons between normalized lesion volume in sensory and motor tracts were not significant however, other than for patients with an MSSS score between 5.0 and 6.0 ($P < 0.05$).

Discussion

In this study, we explored the spatial distribution of multiple sclerosis lesions in the cervical spine by producing voxelwise lesion frequency maps with non-parametric permutation based cluster analyses. In seeking to further understand the contribution of lesion location, we also examined the extent of lesion damage in several regions of interest. We measured the absolute lesion volume, as well as normalized lesion volumes, representing the proportion of the respective regions affected by lesions to account for differences in tissue volume and changing cross-sectional area across the cervical cord. Throughout this work, we confirmed findings (Fog, 1950; Tartaglino *et al.*, 1995; Kearney *et al.*, 2016; Valsasina *et al.*, 2018),



and extended prior works by using atlas-based methods and evaluating differences between patients categorized by clinical subtype and disability measures in a large, multi-centre cohort.

Association between lesion distribution and clinical subtype

Our results showed differences in lesion distribution between clinical subtypes. Whilst lesions occurred frequently in the dorsal column for all subtypes, lesions occurred more than twice as often in the lateral funiculi for primary progressive and secondary progressive patients, compared to relapsing-remitting patients. To further support this finding, absolute and normalized lesion volumes confirmed that the lateral funiculi was more affected by lesions in progressive subtypes. One recent study reported similar results in that primary progressive patients were more likely to incur a lesion in the lateral funiculi, than relapsing-remitting

(Valsasina *et al.*, 2018). From a clinical perspective, lesions affecting the lateral funiculi which are primarily composed of motor pathways may be expected to have a more severe impact on motor function and therefore may at least partially account for the higher disability shown in progressive subtypes. Further analyses to investigate association between lateral lesion presentation and disability in progressive subtypes were not performed in this study, however, and therefore the extent of the contribution, if any, cannot be substantiated from these findings alone.

It was also observed that PPMS patients were also twice as affected by lesions than relapsing-remitting in the central region of cord, which may be considered as cervical grey matter. In line with this, the difference between normalized lesion volume in white and grey matter was lowest in primary progressive patients compared to other phenotypes. Studies have suggested that grey matter may have a relatively poor ability to remyelinate in comparison to white matter (Gilmore *et al.*, 2006), which may explain the higher occurrence of grey matter lesions observed in primary

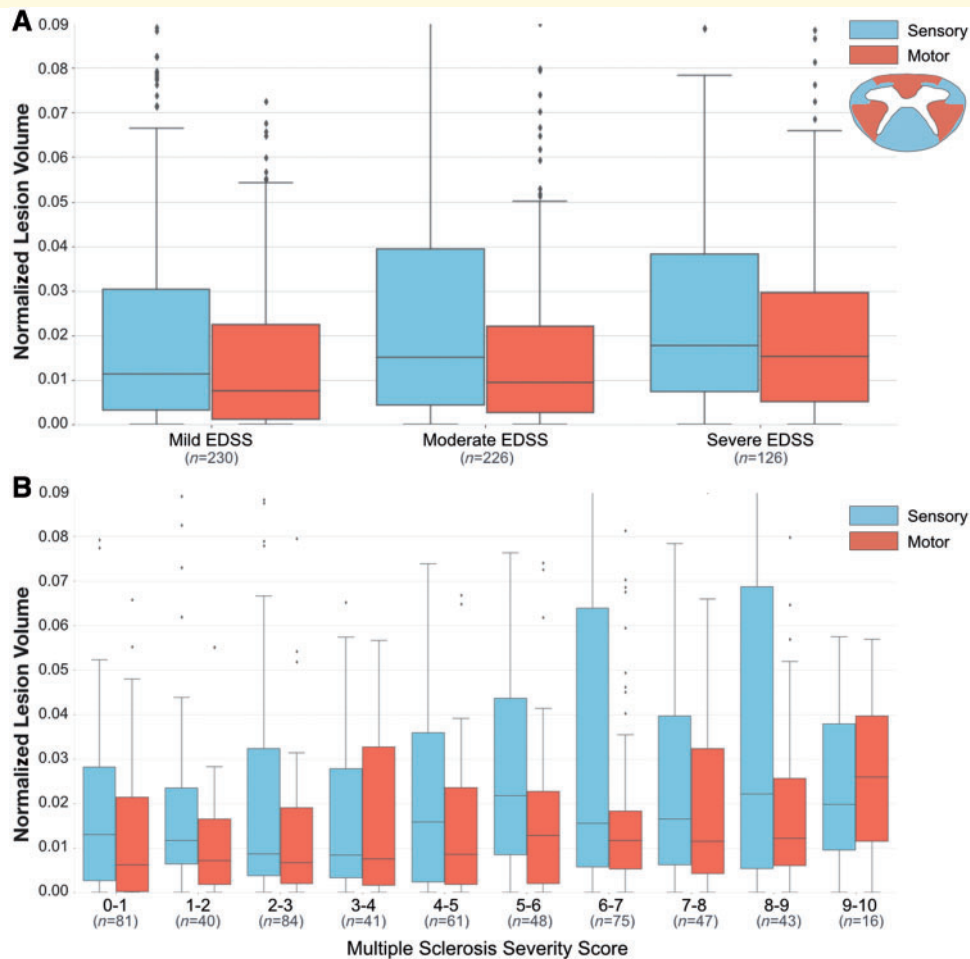


Figure 6 Normalized lesion volumes in cervical spine sensory and motor tracts. Normalized lesion volumes for patient groups categorized by **(A)** EDSS score categories, and **(B)** ranges of MSSS score. Normalized lesion volumes represent the proportion of a region affected by lesions. EDSS scores categories: mild (0–2.5), moderate (3–5.5) and severe (≥ 6). Box and whisker plots represent median, inter-quartile range and range.

progressive patients. Unfortunately, confirmation and comparison of these findings were prevented by the lack of MRI studies identifying differences in the lesion distribution between phenotypes. There are also difficulties present in directly comparing with histopathological studies where patients have often suffered from a long disease duration or severe disease course. This highlights the contribution and need for large MRI studies.

The differences observed between phenotypic distributions were primarily located at cervical vertebral level C3. This may simply be explained by the overall higher lesion presentation found at the C3 vertebral level, which is consistent with previous reports (Valsasina *et al.*, 2018). We also observed that the upper cervical cord was more impacted by lesions than the lower cervical cord in all patient groups, also in line with previous findings in MRI studies (Bonek *et al.*, 2007; Goldin and Kantor, 2008a; Hua *et al.*, 2015; Valsasina *et al.*, 2018) and histopathological studies (DeLuca *et al.*, 2004). However, these observations in the

upper cervical cord may be biased by imaging-related drawbacks in the lower cervical cord, including lesser receive-coil coverage and larger respiratory-related B_0 field variations (Verma and Cohen-Adad, 2014).

Association between lesion distribution and disability measures

To further our investigations, we evaluated patients characterized by disability measures. We found that lesion frequency was significantly associated with EDSS score when correcting for disease duration, in the lateral funiculi and central cervical spine regions. More specifically, these regions were the central area and lateral funiculi of cervical vertebral levels C1 and C3, and the lateral funiculi in C2, C4 and C5. In a similar study, EDSS was also found to correlate in the central region, at cervical level C2 (Valsasina *et al.*, 2018), although no other locations were found to be associated in this study.

Next we evaluated patients characterized by disability measures and found that lesion frequency was significantly correlated with an increasing EDSS score in several cervical spine regions. These regions included the central area and lateral funiculi of cervical vertebral levels C1, C2 and C3, and the lateral funiculi in C4 and C5. In one study, EDSS was also found to correlate in the central region at cervical level C2 (Valsasina *et al.*, 2018), although no other locations were found to be associated in this study.

We also analysed lesion distribution in patients grouped by EDSS score, and further subgrouped by disease duration which showed interesting results. Contrary to expectation, highest lesion frequencies were observed in moderately or severely impaired patients with short disease durations, rather than patients with long disease durations. This observation demonstrates the importance of both clinical factors, in that lesions did not necessarily occur more frequently in patients with a higher EDSS score or longer disease duration, but rather patients with a more aggressive disease course.

Similar to phenotypic observations, lesions commonly affected the dorsal column in most groups. Patients with moderate or severe EDSS scores were more affected by lesions in central and lateral regions with shorter disease durations, indicating that it may be a combination of lesion accumulation and lesion location that contribute to a more severe disease course. Even within a given disease duration category, it was shown that central and lateral regions were more affected by lesions with increase in EDSS score.

These regions, the central and lateral aspects of the cervical cord, which were also frequently affected in patients with progressive subtypes, may be important in better understanding the association between lesions and clinical status. The central cord area, which may be considered as representative of grey matter, has been shown to be a clinically relevant site in studies suggesting that lesions in the cervical grey matter have considerable functional consequences on motor, sensory and bladder dysfunction (Rovaris *et al.*, 2002; Agosta *et al.*, 2007). As for the lateral regions, the prevalence and impact of lesions appearing in these regions has been highlighted in previous MRI (Zackowski *et al.*, 2009) and histopathology studies (Fog, 1950; Oppenheimer, 1978; Nijeholt *et al.*, 2001). Interestingly, the lateral funiculi is primarily composed of motor pathways. However, the correlation between EDSS and normalized motor and sensory tracts, corrected for several clinical factors including disease duration, was surprisingly modest. Correlation coefficients were almost identical between sensory and motor tracts, which is likely explained by the fact that EDSS score is representative of impairment in several functional systems. Other considerations of the EDSS score, particular to this study, are that the measure is reflective of both brain and spinal cord lesions, and is also intended primarily for longitudinal studies. In this instance, it would be suggested to use other scores such the Multiple Sclerosis Functional Composite

(Fischer *et al.*, 1999). This limitation, however, was partially overcome by use of the MSSS score, although it cannot entirely overcome the lack of specificity in the scoring system. The use of the MSSS score did not return results any more informative than those where EDSS score was corrected for disease duration.

Technical considerations

MRI data acquisition

Limitations in this study include variation in MRI data and image quality arising from non-uniform protocol across multiple acquisition sites, which may have led to differences in lesions identification across sites. Conversely, intersite variation also has its advantages in that it minimises bias that may be present in single-site studies.

Other issues include the occurrence of partial cervical spine coverage in some axial scans leading to reliance on sagittal scans, which were shown to be less superior for lesion detectability and is greater impacted by partial volume effect (Breckwoldt *et al.*, 2017). To avoid overestimation of lesion size caused by poor resolution, a weighting was applied to lesions detected in sagittal images, although may have contributed to a lesser occurrence of lesions appearing in lower cervical levels shown throughout this study. With this in mind, previous studies have also shown that lesions are less common in lower levels (Rocca *et al.*, 2013; Hua *et al.*, 2015; Valsasina *et al.*, 2018).

While use of T₂-weighted sequences are considered sufficient in lesion detection, other sequences have shown better lesion contrast, such as the 3D MPRAGE in the cervical spinal cord (Nair *et al.*, 2013; Valsasina *et al.*, 2018). Development of column-specific imaging methods may also be of interest in future studies (Zackowski *et al.*, 2009). High field strength scanners used in this study, operating at 3 T and 7 T, are known to increase the sensitivity and detectability of multiple sclerosis lesions over lower field strength scanners (Dula *et al.*, 2016). Difficulties are, however, still present in detecting lesions in grey matter using conventional MRI. Despite removing T₂*-weighted data from analyses involving grey matter, these difficulties could not be entirely overcome, which may explain minor discrepancies between our study and histopathological studies where higher proportions of lesions were observed in grey matter over white matter (Gilmore *et al.*, 2009a). Use of grey matter specific pulse sequences such as double inversion recovery or phase sensitive recovery (Kilsdonk *et al.*, 2016), as well as exclusive use of 7 T scanners, which has also been approved for clinical use, has been suggested to overcome contrast issues between lesions and grey matter (Mainero *et al.*, 2009; Beck *et al.*, 2018).

MRI data processing

Common to multiple sclerosis template-based studies, poor registration between subject and template spaces causes misplacement of lesions and subsequent inaccuracies in

lesion quantification. To mitigate this issue, spinal cord masks were used as a preliminary guide in the non-linear registration, instead of the scans themselves which are often hampered by lesions and artifact causing misregistration (De Leener *et al.*, 2016; Paquin *et al.*, 2018). Visual inspection was also performed, and good similarity was shown in our study between native and template space measures.

The benefits of registering data to a spinal cord template outweigh potential inaccuracies associated with registration, due to the ability of using atlas-based as opposed to manually-drawn masks for delineating white matter tracts (De Leener *et al.*, 2016). Other methods attempt to manually draw masks for delineating spinal tracts and regions based on personal interpretation and user knowledge of cord anatomy (Zackowski *et al.*, 2009; Kearney *et al.*, 2013; Hua *et al.*, 2015), or ignore anatomically-defined regions (Valsasina *et al.*, 2012; Breckwoldt *et al.*, 2017). Partial volume effect, which remains a frequent challenge in spinal MRI studies, is also of less concern in probabilistic atlas-based methods since Gaussian-mixture models can retrieve the true metric values within tracts (Lévy *et al.*, 2015).

Consistent with histopathological studies, we observed that lesions most frequently occurred in the central portions of white matter columns, in all patient groups (Fog, 1950). This observation has been previously described as lesions originating where white matter is broadest, most commonly at the centre of the lateral regions and at the posterior median sulcus. The phenomenon now known as central vein sign describes lesion formation around the veins (Sati *et al.*, 2016), which prompts investigation into the venous anatomy of the spinal cord.

Further perspectives

Throughout this study we focused on lesions in the cervical cord, which although showed interesting results, excludes lesions existing in the brain. The PAM50 spinal cord template has been aligned with the ICBM152 space (De Leener *et al.*, 2018), enabling combination of brain and spinal MRI, and therefore prompting further investigation into influence of brain and cervical spine lesion location on clinical status. Recent progress in automatic multiple sclerosis lesion segmentation in the spinal cord (Gros *et al.*, 2018), which has shown good performance across highly variable MRI data, may also be of interest in follow-up studies. Addressing other key pathological mechanisms, such as atrophy and myelopathy, may increase the strength of correlation between lesion measures and disability, as has been shown previously (Lukas *et al.*, 2013; Rocca *et al.*, 2013; Kearney *et al.*, 2015a). Finally, performing a similar longitudinal study is likely to considerably improve our understanding of the association between lesion location and clinical status.

Conclusion

In this study we produced an automatic processing and analysis pipeline which has been made publicly available,

minimizing user bias and promoting standardization and reproducibility of scientific results. We used voxelwise lesion frequency maps and atlas-based method to characterize cervical spine lesion distribution in a large multicentre cohort of multiple sclerosis patients with high precision. We found that the lateral funiculi and central cord area were significantly more affected by lesions in progressive subtypes than relapsing subtypes, and are also associated with disability.

Acknowledgements

The authors thank Nikola Stikov, Gabriel Mangeat, Nala Kangoo and Percy McDonald for fruitful discussions. The following people are acknowledged for sharing data: Bailey Lyttle, Ben Conrad and Bennett Landman (Vanderbilt University); Marie-Pierre Ranjeva (CHU Timone); OFSEP participants: Roxana Ameli, Gildas Bonhomme, Pierre-Laurent Bonnier, Claire Boutet, Bruno Brochet, Jean-Philippe Camdessanche, Olivier Casez, Béatrice Claise, Pierre Clavelou, François Cotton, Jérôme De Seze, Vincent Dousset, Jean-François Dugor, Jean-Christophe Ferre, Sylvie Grand, Alexandre Krainik, Stéphane Kremer, Nicolas Menjot De Champfleu, Jean-Amédée Roch, Thomas Tourdias, Sandra Vukusic. This study was supported by researchers at the National Institute for Health Research University College London Hospitals Biomedical Research Centre.

Funding

Funded by the Canada Research Chair in Quantitative Magnetic Resonance Imaging, CIHR-FDN-143263, FRQS-28826, FRQNT-2015-PR-182754, NSERC-435897-2013, QBIN, NMSS RG-1501-02840 (S.A.S.), NIH/NINDS R21 NS087465-01 (S.A.S.), NIH/NEI R01 EY023240 (S.A.S.), DoD W81XWH-13-0073 (S.A.S.), the Intramural Research Program of NIH/NINDS (J.L., D.S.R., G.N.), PHRC (EMISEP), NIH/NINDS R01 NS078322-02 (C.M.), ClinicalTrials.gov (NCT02117375), CNRS, “Fondation A*midex-Investissements d’Avenir”, the Stockholm County Council (ALF grant 20150166), Swedish Society for Medical Research (T.G.), Guarantors of Brain (F.P.), ANR-10-COHO-002, OFSEP, EDMUS Foundation against multiple sclerosis, UK MS Society and the National Institute for Health Research University College London Hospitals Biomedical Research Centre, EMD Serono (C.M., R.B.).

Competing interests

M.F. is Editor-in-Chief of the Journal of Neurology; received compensation for consulting services and/or speaking activities from Biogen Idec, Merck-Serono, Novartis, Teva Pharmaceutical Industries; and receives research

support from Biogen Idec, Merck-Serono, Novartis, Teva Pharmaceutical Industries, Roche, Italian Ministry of Health, Fondazione Italiana Sclerosi Multipla, and ARiSLA (Fondazione Italiana di Ricerca per la SLA). J.H. has received honoraria for serving on advisory boards for Biogen, Sanofi-Genzyme and Novartis; and speaker's fees from Biogen, Novartis, Merck-Serono, Bayer-Schering, Teva and Sanofi-Genzyme; and has served as P.I. for projects or received unrestricted research support from Biogen Idec, Merck-Serono, TEVA, Sanofi-Genzyme and Bayer-Schering. M.A.R. received speaker honoraria from Biogen Idec, Novartis, Genzyme, Sanofi-Aventis, Teva and Merck Serono and receives research support from the Italian Ministry of Health and Fondazione Italiana Sclerosi Multipla. P.V. received speaker honoraria from Biogen Idec, Novartis and ExceMED. R.B. has received consulting fees from Bayer, EMD Serono, Genentech, Guerbet, Sanofi-Genzyme, and Shire and research support from EMD Serono and Sanofi-Genzyme. S.N. reports personal fees from NeuroRx Research, a speaker's honorarium from Novartis Canada, and grants from the Canadian Institutes of Health Research, unrelated to the submitted work. J.P. received speaker honoraria from Biogen, Roche, Genzyme, Novartis, and research supports from the French Ministry of Health and ARSEP. O.C. receives grant support from the UK MS Society, National MS Society, NIHR, EU-H2020, Spinal Cord Research Foundation, Rosetrees Trust, Progressive MS Alliance, Bioclinica AND GE Neuro. She is a consultant for Novartis, Teva, Roche, Biogen, and Merck-Serono. She is an Associate Editor of *Neurology*, for which she receives and honorarium. E.C. has received consulting fees from Biogen and Novartis.

Supplementary material

Supplementary material is available at *Brain* online.

References

- Absinta M, Sati P, Reich DS. Advanced MRI and staging of multiple sclerosis lesions. *Nat Rev Neurol* 2016; 12: 358–68.
- Agosta F, Pagani E, Caputo D, Filippi M. Associations between cervical cord gray matter damage and disability in patients with multiple sclerosis. *Arch Neurol* 2007; 64: 1302–5.
- Arrambide G, Rovira A, Sastre-Garriga J, Tur C, Castelló J, Río J, et al. Spinal cord lesions: a modest contributor to diagnosis in clinically isolated syndromes but a relevant prognostic factor. *Mult Scler* 2018; 24: 301–12.
- Beck ES, Sati P, Sethi V, Kober T, Dewey B, Bhargava P, et al. Improved visualization of cortical lesions in multiple sclerosis using 7T MP2RAGE. *AJNR Am J Neuroradiol* 2018; 39: 459–66.
- Bonek R, Orlicka K, Maciejek Z. Demyelinating lesions in the cervical cord in multiple sclerosis 10 years after onset of the disease. Correlation between MRI parameters and clinical course. *Neurol Neurochir Pol* 2007; 41: 229–33.
- Breckwoldt MO, Gradl J, Hähnel S, Hielscher T, Wildemann B, Diem R, et al. Increasing the sensitivity of MRI for the detection of multiple sclerosis lesions by long axial coverage of the spinal cord: a prospective study in 119 patients. *J Neurol* 2017; 264: 341–9.
- Brownlee WJ, Altmann DR, Alves Da Mota P, Swanton JK, Miszkiel KA, Wheeler-Kingshott CG, et al. Association of asymptomatic spinal cord lesions and atrophy with disability 5 years after a clinically isolated syndrome. *Mult Scler* 2017; 23: 665–74.
- Commowick O, Istace A, Kain M, Laurent B, Leray F, Simon M, et al. Objective evaluation of multiple sclerosis lesion segmentation using a data management and processing infrastructure. *Sci Rep* 2018; 8: 13650.
- De Leener B, Fonov VS, Collins DL, Callot V, Stikov N, Cohen-Adad J. PAM50: unbiased multimodal template of the brainstem and spinal cord aligned with the ICBM152 space. *Neuroimage* 2018; 165: 170–9.
- De Leener B, Kadoury S, Cohen-Adad J. Robust, accurate and fast automatic segmentation of the spinal cord. *Neuroimage* 2014; 98: 528–36.
- De Leener B, Lévy S, Dupont SM, Fonov VS, Stikov N, Louis Collins D, et al. SCT: Spinal Cord Toolbox, an open-source software for processing spinal cord MRI data. *Neuroimage* 2016; 145: 24–43.
- DeLuca GC, Ebers GC, Esiri MM. Axonal loss in multiple sclerosis: a pathological survey of the corticospinal and sensory tracts. *Brain* 2004; 127: 1009–18.
- Dice LR. Measures of the amount of ecologic association between species. *Ecology* 1945; 26: 297–302.
- Dula AN, Pawate S, Dortch RD, Barry RL, George-Durrett KM, Lyttle BD, et al. Magnetic resonance imaging of the cervical spinal cord in multiple sclerosis at 7T. *Mult Scler* 2016; 22: 320–8.
- Fazekas F, Barkhof F, Filippi M, Grossman RI, Li DK, McDonald WI, et al. The contribution of magnetic resonance imaging to the diagnosis of multiple sclerosis. *Neurology* 1999; 53: 448–56.
- Filippi M, Bozzali M, Horsfield MA, Rocca MA, Sormani MP, Iannucci G, et al. A conventional and magnetization transfer MRI study of the cervical cord in patients with MS. *Neurology* 2000; 54: 207.
- Filippi M, Rocca MA. Conventional MRI in multiple sclerosis. *J Neuroimaging* 2007; 17 (Suppl 1): 3S–9S.
- Fischer JS, Rudick RA, Cutter GR, Reingold SC. The multiple sclerosis functional composite. *Mult Scler* 1999; 5.
- Fog T. Topographic distribution of plaques in the spinal cord in multiple sclerosis. *Arch Neurol Psychiatry* 1950; 63: 382–414.
- Gass A, Rocca MA, Agosta F, Ciccarelli O, Chard D, Valsasina P, et al. MRI monitoring of pathological changes in the spinal cord in patients with multiple sclerosis. *Lancet Neurol* 2015; 14: 443–54.
- Gilmore CP, Bö L, Owens T, Lowe J, Esiri MM, Evangelou N. Spinal cord gray matter demyelination in multiple sclerosis—a novel pattern of residual plaque morphology. *Brain Pathol* 2006; 16: 202–8.
- Gilmore CP, Donaldson I, Bö L, Owens T, Lowe J, Evangelou N. Regional variations in the extent and pattern of grey matter demyelination in multiple sclerosis: a comparison between the cerebral cortex, cerebellar cortex, deep grey matter nuclei and the spinal cord. *J Neurol Neurosurg Psychiatry* 2009a; 80: 182–7.
- Gilmore CP, Geurts JJ, Evangelou N, Bot JC, van Schijndel RA, Pouwels PJ, et al. Spinal cord grey matter lesions in multiple sclerosis detected by post-mortem high field MR imaging. *Mult Scler* 2009b; 15: 180–8.
- Goldin GH, Kantor D. Distribution of multiple sclerosis plaques in the spinal cord. In: *Multiple Sclerosis*. London, England: Sage Publications LTD; 2008a. p. S110.
- Goldin G, Kantor D. Distribution of multiple sclerosis plaques in the spinal cord. *Mult Scler* 2008b; 14: S110.
- Gros C, De Leener B, Badji A, Maranzano J, Eden D, Dupont SM, et al. Automatic segmentation of the spinal cord and intramedullary multiple sclerosis lesions with convolutional neural networks. *Neuroimage* 2018; 184: 901–15.
- Gros C, De Leener B, Dupont SM, Martin AR, Fehlings MG, Bakshi R, et al. Automatic spinal cord localization, robust to MRI contrasts using global curve optimization. *Med Image Anal* 2017; 44: 215–27.

- Hua LH, Donlon SL, Sobhanian MJ, Portner SM, Okuda DT. Thoracic spinal cord lesions are influenced by the degree of cervical spine involvement in multiple sclerosis. *Spinal Cord* 2015; 53: 520–5.
- Jenkinson M, Beckmann CF, Behrens TEJ, Woolrich MW, Smith SM. FSL. *Neuroimage* 2012; 62: 782–90.
- Kaunzner UW, Gauthier SA. MRI in the assessment and monitoring of multiple sclerosis: an update on best practice. *Ther Adv Neurol Disord* 2017; 10: 247–61.
- Kearney H, Altmann DR, Samson RS, Yiannakas MC, Wheeler-Kingshott CAM, Ciccarelli O, et al. Cervical cord lesion load is associated with disability independently from atrophy in MS. *Neurology* 2015a; 84: 367–73.
- Kearney H, Miller DH, Ciccarelli O. Spinal cord MRI in multiple sclerosis—diagnostic, prognostic and clinical value. *Nat Rev Neurol* 2015b; 11: 327–38.
- Kearney H, Miszkil KA, Yiannakas MC, Altmann DR, Ciccarelli O, Miller DH. Grey matter involvement by focal cervical spinal cord lesions is associated with progressive multiple sclerosis. *Mult Scler* 2016; 22: 910–20.
- Kearney H, Miszkil KA, Yiannakas MC, Ciccarelli O, Miller DH. A pilot MRI study of white and grey matter involvement by multiple sclerosis spinal cord lesions. *Mult Scler Relat Disord* 2013; 2: 103–8.
- Kidd D, Thorpe JW, Thompson AJ, Kendall BE, Moseley IF, MacManus DG, et al. Spinal cord MRI using multi-array coils and fast spin echo. II. Findings in multiple sclerosis. *Neurology* 1993; 43: 2632–7.
- Kilsdonk ID, Jonkman LE, Klaver R, van Veluw SJ, Zwanenburg JJM, Kuijer JPA, et al. Increased cortical grey matter lesion detection in multiple sclerosis with 7 T MRI: a post-mortem verification study. *Brain* 2016; 139: 1472–81.
- Kurtzke JF. Rating neurologic impairment in multiple sclerosis: an expanded disability status scale (EDSS). *Neurology* 1983; 33: 1444–52.
- Lévy S, Benhamou M, Naaman C, Rainville P, Callot V, Cohen-Adad J. White matter atlas of the human spinal cord with estimation of partial volume effect. *Neuroimage* 2015; 119: 262–71.
- Lukas C, Sombekke MH, Bellenberg B, Hahn HK, Popescu V, Bendfeldt K, et al. Relevance of spinal cord abnormalities to clinical disability in multiple sclerosis: MR imaging findings in a large cohort of patients. *Radiology* 2013; 269: 542–52.
- Lycklama G, Thompson A, Filippi M, Miller D, Polman C, Fazekas F, et al. Spinal-cord MRI in multiple sclerosis. *Lancet Neurol*. 2003; 2: 555–62.
- Mainero C, Benner T, Radding A, van der Kouwe A, Jensen R, Rosen BR, et al. In vivo imaging of cortical pathology in multiple sclerosis using ultra-high field MRI. *Neurology* 2009; 73: 941–8.
- Nair G, Absinta M, Reich DS. Optimized T1-MPRAGE sequence for better visualization of spinal cord multiple sclerosis lesions at 3T. *AJNR Am J Neuroradiol* 2013; 34: 2215–22.
- Nijeholt GJ, Bergers E, Kamphorst W, Bot J, Nicolay K, Castelijns JA, et al. Post-mortem high-resolution MRI of the spinal cord in multiple sclerosis: a correlative study with conventional MRI, histopathology and clinical phenotype. *Brain* 2001; 124: 154–66.
- Nijeholt GJ, van Walderveen MA, Castelijns JA, van Waesberghe JH, Polman C, Scheltens P, et al. Brain and spinal cord abnormalities in multiple sclerosis. Correlation between MRI parameters, clinical subtypes and symptoms. *Brain* 1998; 121 (Pt 4): 687–97.
- Oppenheimer DR. The cervical cord in multiple sclerosis. *Neuropathol Appl Neurobiol* 1978; 4: 151–62.
- Paquin M-È, El Mendili MM, Gros C, Dupont SM, Cohen-Adad J, Pradat P-F. Spinal cord gray matter atrophy in amyotrophic lateral sclerosis. *AJNR Am J Neuroradiol* 2018; 39: 184–92.
- Rocca MA, Valsasina P, Damjanovic D, Horsfield MA, Mesaros S, Stosic-Opincal T, et al. Voxel-wise mapping of cervical cord damage in multiple sclerosis patients with different clinical phenotypes. *J Neurol Neurosurg Psychiatry* 2013; 84: 35–41.
- Rovaris M, Bozzali M, Iannucci G, Ghezzi A, Caputo D, Montanari E, et al. Assessment of normal-appearing white and gray matter in patients with primary progressive multiple sclerosis. *Arch Neurol* 2002; 59: 1406–12.
- Rovaris M, Bozzali M, Santuccio G, Iannucci G, Sormani MP, Colombo B, et al. Relative contributions of brain and cervical cord pathology to multiple sclerosis disability: a study with magnetisation transfer ratio histogram analysis. *J Neurol Neurosurg Psychiatry* 2000; 69: 723–7.
- Roxburgh RSHR, Seaman SR, Masterman T, Hensiek AE, Sawcer SJ, Vukusic S, et al. Multiple Sclerosis Severity Score: using disability and disease duration to rate disease severity. *Neurology* 2005; 64: 1144–51.
- Sati P, Oh J, Constable RT, Evangelou N, Guttman CRG, Henry RG, et al. The central vein sign and its clinical evaluation for the diagnosis of multiple sclerosis: a consensus statement from the North American Imaging in Multiple Sclerosis Cooperative. *Nat Rev Neurol* 2016; 12: 714–22.
- Schmierer K, McDowell A, Petrova N, Carassiti D, Thomas DL, Miquel ME. Quantifying multiple sclerosis pathology in post mortem spinal cord using MRI. *Neuroimage* 2018; 182: 251–8.
- Smith SM, Jenkinson M, Woolrich MW, Beckmann CF, Behrens TEJ, Johansen-Berg H, et al. Advances in functional and structural MR image analysis and implementation as FSL. *Neuroimage* 2004; 23: S208–19.
- Smith SM, Nichols TE. Threshold-free cluster enhancement: addressing problems of smoothing, threshold dependence and localisation in cluster inference. *Neuroimage* 2009; 44: 83–98.
- Sombekke MH, Wattjes MP, Balk LJ, Nielsen JM, Vrenken H, Uitdehaag BMJ, et al. Spinal cord lesions in patients with clinically isolated syndrome: a powerful tool in diagnosis and prognosis. *Neurology* 2013; 80: 69–75.
- Stankiewicz JM, Neema M, Alsop DC, Healy BC, Arora A, Buckle GJ, et al. Spinal cord lesions and clinical status in multiple sclerosis: A 1.5 T and 3 T MRI study. *J Neurol Sci* 2009; 279: 99–105.
- Stroman PW, Wheeler-Kingshott C, Bacon M, Schwab JM, Bosma R, Brooks J, et al. The current state-of-the-art of spinal cord imaging: methods. *Neuroimage* 2014; 84: 1070–81.
- Tartaglino LM, Friedman DP, Flanders AE, Lublin FD, Knobler RL, Liem M. Multiple sclerosis in the spinal cord: MR appearance and correlation with clinical parameters. *Radiology* 1995; 195: 725–32.
- Valsasina P, Aboulwafa M, Preziosa P, Messina R, Falini A, Comi G, et al. Cervical Cord T1-weighted hypointense lesions at MR imaging in multiple sclerosis: relationship to cord atrophy and disability. *Radiology* 2018; 288: 234–44.
- Valsasina P, Horsfield MA, Rocca MA, Absinta M, Comi G, Filippi M. Spatial normalization and regional assessment of cord atrophy: voxel-based analysis of cervical cord 3D T1-weighted images. *AJNR Am J Neuroradiol* 2012; 33: 2195–200.
- Verma T, Cohen-Adad J. Effect of respiration on the B0 field in the human spinal cord at 3T. *Magn Reson Med* 2014; 72: 1629–36.
- Weier K, Mazraeh J, Naegelin Y, Thoeni A, Hirsch JG, Fabbro T, et al. Biplanar MRI for the assessment of the spinal cord in multiple sclerosis. *Mult Scler* 2012; 18: 1560–9.
- Yushkevich PA, Piven J, Hazlett HC, Smith RG, Ho S, Gee JC, et al. User-guided 3D active contour segmentation of anatomical structures: significantly improved efficiency and reliability. *Neuroimage* 2006; 31: 1116–28.
- Zackowski KM, Smith SA, Reich DS, Gordon-Lipkin E, Chodkowski BA, Sambandan DR, et al. Sensorimotor dysfunction in multiple sclerosis and column-specific magnetization transfer-imaging abnormalities in the spinal cord. *Brain* 2009; 132: 1200–9.